Pure & Appl. Chem., Vol. 46, pp. 127–134. Pergamon Press, 1976. Printed in Great Britain.

ON PRESENT THEORIES OF THE CONDENSED POLYMER STATE

W. PECHHOLD, E. LISKA, H. P. GROSSMANN and P. C. HÄGELE
University of Ulm, Abteilung Experimentelle Physik II, FRG

Abstract—An improvement of the bundle model gives the possibility to discuss quantitatively the solid state transition and the final melting of PE and calculate the transition data as well as the cooperativity. A similar quantitative treatment is carried out to explain the kink-block transitions in clay organic complexes.

As we all know, there is no chance today to achieve any quantitative molecular-based result by strictly applying the fundamental laws of physics to a many-body disordered system, like fluids, melts or the amorphous solid state. What we have to introduce are assumptions which allow the problem to be treated analytically or at least numerically. Each assumption is part of a model, and one should in fact look upon models not only regarding their drawings but also by examining the physical assumptions involved, because these are essential for a quantitative application of a model.

The most serious assumption to be made for a system of condensed polymer-chains is the degree of order or chain alignment. The models proposed so far differ therefore in the assumed content of chain parallelism (Fig. 1).

(1) The random coil model—established for dilute solutions—in which one has to envisage densely-packed and mutually penetrating coiled molecules.[1] To achieve a dense package, however, a certain number of chain segments have to be parallel, a condition which possibly violates the basic assumption of this model.

(2) The bead-string model—qualitatively proposed by Schoon[2]—in which molecules pass from one folded region to another.

(3) The meander model—in which bundles of molecules sharply fold, to give an isotropic and densely-packed polymer material.[3] This model comes closest to the bundle concept of Kargin which he proposed in 1957.[4]

There are two more micellar models to be mentioned.

(4) The folded-chain fringed micellar grain model by Yeh[5] which combines bundle domains with partially folded grain boundaries and intergrain regions in which the molecules are in a more truly random conformation.

(5) The cell structure model of polymer gels by Vollmert[6] in which only partial penetration of neighbouring coiled molecules into their contact zones is required from side group conversion experiments.

Three of these models have been proposed only qualitatively to account for certain experimental results, e.g. electron diffraction and microscopy. A quantitative treatment will possibly give rise to difficulties.

The random coil model and the meander model represent opposite views. Considering the chain alignment they are limiting models. Though differing greatly, both can in many cases explain the same experimental results, e.g. rubber-elasticity, the radius of gyration, measured by neutron scattering[7,8] and the magnetic birefringence.[9,10]

Since the discussion of the most recent experimental results on the basis of either model is going on, we will not deal with any details here, but only draw attention to recent electron microscopic work by Petermann and Gleiter.[11–13] These authors investigated thin polyethylene films—prepared by a spreading technique onto a surface of a hot liquid—and concluded, that the random coil model could not explain most of their observations. So, at least for thin films, 100–1000 Å in thickness, the bundle model seems favoured by these experiments. Now turning to the theoretical approach within the framework of the two models, it is obvious that either model is based on fundamental assumptions which have not been proved so far. The random coil concept assumes the neighbouring molecules to set up a mean field similar to the θ-condition in dilute solution and does not take into account contributions of energy from local distortions of molecules which certainly arise from the mutual penetration.[1]

The bundle model—as proposed by Blasenbrey and Pechhold[14] starts from the ideal crystal and describes the real crystal by introducing appropriate defects (kink-isomers). In order to explain the short range order of the melt or the amorphous state it assumes the crystal order to be destroyed by increasing the concentration of kink-isomers, the chains, however, remaining nearly parallel. A second assumption is made in the course of an approximate cooperative treatment by choosing a segment of four CH_2-groups (in the case of PE) as statistical

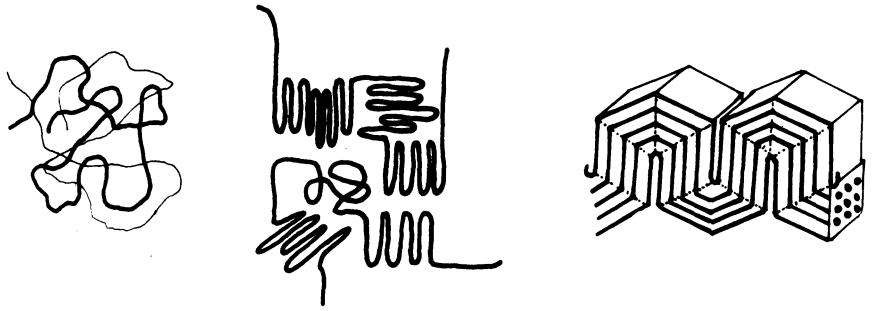

Fig. 1. From left to right: the random coil, the bead-string, and the meander model.

element which predetermines the final kink density of the melt.

In the following we shall neither discuss further details of these models nor present corresponding theories of polymer properties. Instead we limit ourselves to derive an improvement of the bundle model as far as it applies to the problem of molecular order and to phase transitions.

This improvement has been stimulated—as progress in theory often is—by a new experimental fact: the observation of a high pressure crystalline phase in PE by Bassett and coworkers.[15,16] This hexagonal phase, showing a sharp Debye–Scherrer ring ($a = 8.46$ Å, $b = 4.88$ Å compared with $a = 7.58$ Å, $b = 4.81$ Å for the all trans-crystal at 220°C and about 4 kbar), has consumed about 3/4 of the heat of melting and 1/2 of the volume change at melting (at 5 kbar) and is observed above 3 kbar.

This phase corresponds to the crystalline high temperature phase in trans-PBD and probably to similar phases in other polymers. Such phases, which probably have incorporated a lot of conformational entropy but remain crystalline (at least laterally) and therefore densely packed, can be explained by any theory which claims to describe melting.

Before giving a thermodynamical treatment, we detail the method to be used on another example, namely the formation of kink-block structures in clay organic complexes that were extensively investigated by Lagaly and Weiss.[17,18] These observations are of great importance for membrane research too.

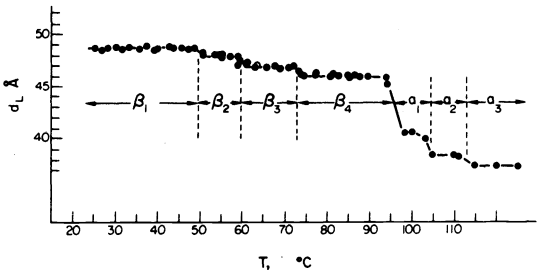

Fig. 3. Temperature dependency of the basal spacings d_L of *n*-tetradecylammonium-tetradecanol-beidellite showing the stability ranges of the low temperature phases $\beta_1, \beta_2, \beta_3, \beta_4$ and of the high temperature phases $\alpha_1, \alpha_2, \alpha_3$. (from[18]).

KINK-BLOCK FORMATION IN CLAY ORGANIC COMPLEXES

Figure 2 shows a system of bilayers formed by alkylammonium and alkanol chains prepared by cation exchange in a beidellite crystal. Studying the temperature dependence of the long spacing, Weiss and Lagaly found several phase transitions mostly accompanied by 1.3 Å steps in lamella height (Fig. 3). The authors showed that the only explanation left is the formation of kink blocks.

Figure 4 shows a Stuart-model of one half of a bilayer between rigid plates indicating the kink-blocks formed. After the formation of more than half of the maximum number of kink-blocks the chains are assumed to tilt because of a better packing of the existing blocks. On further increase of temperature the residual kink-blocks are formed.

In order to treat this system statistically, one has to know the partition function Q of a C_2H_4-rotator in trans- and in kink-conformation (Fig. 5). The following rotational potential has been suitable:

$$U(\varphi) = 2.15(1 - \cos\varphi) - 1.17(1 - \cos 2\varphi) + 3.83(1 - \cos 3\varphi)\,\frac{\text{kcal}}{\text{mol}}.$$

From the partition functions (given in Fig. 5) the differences in entropy and enthalpy are calculated in the usual way. One gets for each kink in an isolated chain

$$S_{kink} - S_{trans} = 1.29 \text{ e.u.}, \quad H_{kink} - H_{trans} = 1.27\,\frac{\text{kcal}}{\text{mol}}. \quad (1)$$

The enthalpy per kink in a block has to be reduced by about 0.29 kcal/mol because the available cross-section per chain is 24 Å^2 (due to the layer charge) compared with that of the best intermolecular fit (18.2 Å^2 in PE):

$$(H_{kink}-H_{trans})_{block} = 1.27\text{–}0.29 = 0.98 \text{ kcal/mol}. \quad (1a)$$

Figure 6 shows a drawing of a bilayer with one kink-block and the free energy for such a system per chain pair (in chain direction). This free energy is composed of the molar free energies G_t and G_k of trans- and kink-

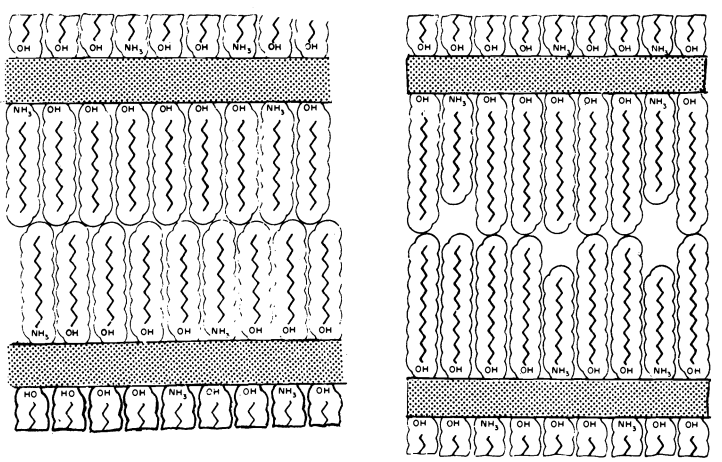

Fig. 2. Bilayers formed by alkylammonium and alkanol chains through cation exchange in beidellite crystal (from[18]).

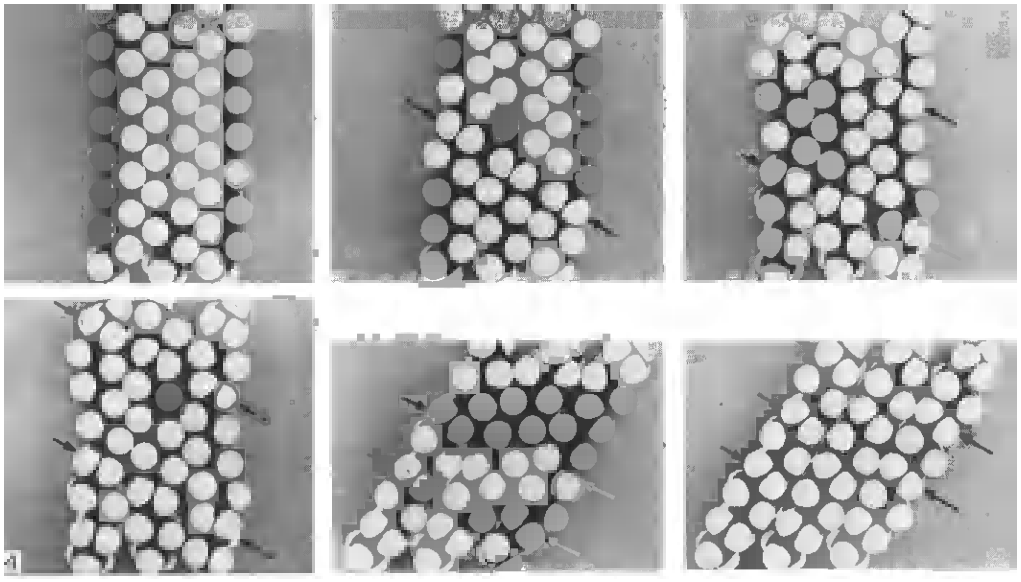

Fig. 4. Stuart model of a monolayer between rigid plates indicating the kink-blocks formed.

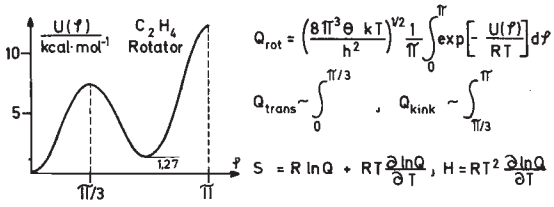

Fig. 5. Calculation of entropy and enthalpy of a hindered rotator in trans- and kink-conformation.

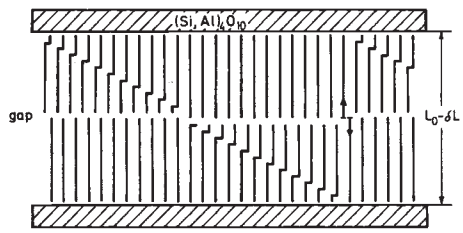

$$G = (1-y)G_t + yG_K - yRT\left[\ln 2 + \frac{c}{L_0}\ln\frac{(n-1)!\left(\frac{L_0}{c}-n+1\right)!}{n!\left(\frac{L_0}{c}-n\right)!}\right]$$
$$+RT\,[y\ln y + (1-y)\ln(1-y)]$$
$$+\frac{1}{2}(1-y)\,f_t(\delta L)^2 + \frac{1}{2}y\,f_K\left(\frac{c}{2}-\delta L\right)^2$$

Fig. 6. Model of bilayer and the free energy of chain pairs (y probability for a kink, $1-y$ for all trans)—full cluster—entropy assumed. $n = 1$ for the first kink-block transition.

conformations respectively multiplied by their probabilities, an additional entropy term yR1n2 which takes into account the equivalent type of kinks with their rotational axis in the second C–C-bond direction, an entropy term accounting for the different possibilities of kink-block arrangements, and the entropy of mixing trans- and kink-conformations. The bottom line (Fig. 6) comprises the cooperativity of the problem and gives the energy of deformation if not all the chain pairs are kinked or unkinked (rigid beidellite-layer!).

The thermodynamic treatment starts with the equilibrium conditions

$$\frac{\partial G}{\partial \delta L} = 0, \quad \frac{\partial G}{\partial y} = 0 \tag{2}$$

which lead to the following equation (with $f_i = f_k = f$)

$$\frac{G_k - G_t}{RT} - \ln 2 - \frac{c}{L_0}\ln\frac{(n-1)!\left(\left(\frac{L_0}{c}-n+1\right)\right)!}{n!\left(\frac{L_0}{c}-n\right)!}$$
$$= \ln\frac{1-y}{y} + B(2y-1). \tag{3}$$

This equation, the right side of which is plotted in Fig. 7 for three different B's, gives the equilibrium kink concentrations as function of temperature in the regions with negative slope. The positive slope in between indicates a region of instability (maxima of G) which the system may overcome by a first order phase transition. As the free energy of the two competing phases—with low and high kink density respectively—must be equal at the transition

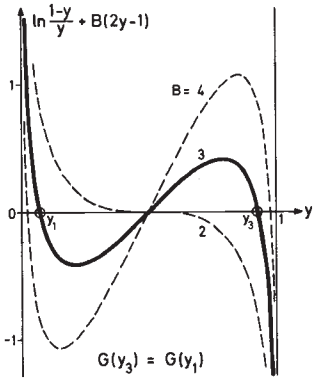

Fig. 7. Thermodynamic analysis of kink-block transition (for details see text).

temperature, this temperature is determined by the left side of the upper equation if its representation (a horizontal line) bisects the area under the S-shaped curve (representing the right side). In this simple symmetric case the left side has to become zero at the transition.

The model of course must also give the cooperativity parameter B, which is an additional test besides yielding the right transition data. In this case

$$B = \frac{f}{2kt}\left(\frac{c}{2}\right)^2 = \frac{1}{2kT(S_{cc}+S_{gap})}\frac{A}{L_0}\left(\frac{c}{2}\right)^2 = 3.4,\ldots,3.0 \quad (4)$$

which is mainly determined by the compliance of the gap between the monolayers. B turns out to be approximately 3 using: $A = 24\ \text{Å}^2$, $S_{cc} = 3.4\times10^{-13}\ \text{cm}^2/\text{dyn}$ and the "gap compliance" $S_{gap}\times L_0 = 1.1\times10^{-18}\ \text{cm}^3/\text{dyn}$, recently measured by Strobl[19] from an analysis of the Raman active accordeon modes in tritriacontane.

From the transition intercepts y_3 and y_1 one gets the jump in kink concentration and the transition data ΔH and ΔS.

$$\Delta H = (y_3 - y_1)(H_{kink} - H_{trans}) = 0.85\times0.98 = 0.83\ \frac{\text{kcal}}{\text{mol}} \quad (5)$$

$$\Delta S = (y_3 - y_1)\left[S_{kink} - S_{trans} + R\ln 2 + R\frac{c}{L_0}\ln\frac{(n-1)!\left(\frac{L_0}{c}-n+1\right)!}{n!\left(\frac{L_0}{c}-n\right)!}\right]. \quad (6)$$

Table 1 gives the results for 3 bilayer systems, which sufficently agree with the experimental data available (given in brackets, compare Fig. 8). Starting with the first kink-block formation ($n = 1$) this statistical treatment has been similarly applied to subsequent kink-block transitions taking into account the reduced entropy of kink-block arrangements along the chains (which is a function of n).

At this stage it must be admitted, that we kept back so far a certain difficulty which arose: We got the free energy G of this bilayer system (Fig. 6) by using the full entropy of mixing kinked and unkinked chains and only considering the formation of kink-blocks in the energy per kink (in which no additional misfit energy was included). In fact, we have made use of a hypothesis which seems to us very important for condensed phase systems and which we call

Cluster-entropy hypothesis

The entropy (e.g. transition-, orientation-, deformation-entropy) of a cluster of m equivalent elements, each having f internal (e.g. vibrational) accessible states is m times the entropy of a single element as long as f is sufficiently larger than m.

In other words, equivalent elements retain their full entropy contribution as long as clusters formed by them contain no more elements than the accessible states of a single element. This hypothesis has still to be proved, but is intuitively plausible if one remembers the definition of microstates as states including all degrees of freedom, not only those of interest in a special problem. There are several applications of this hypothesis in various fields like those of membranes, liquid crystals, condensed polymers and biopolymers.

CRYSTALLINE KINK-BLOCK PHASE IN POLYETHYLENE

Let us now consider the crystalline high pressure phase of PE. From Bassett's X-ray work[16] it follows that the

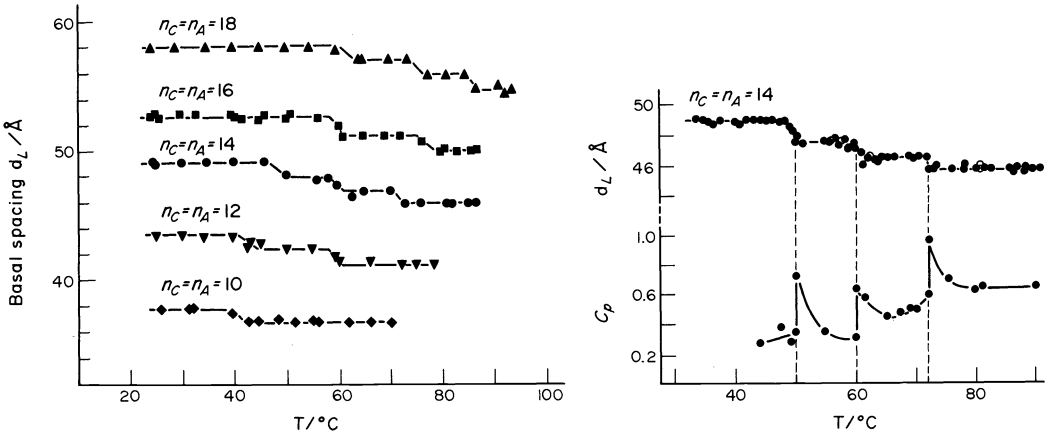

Fig. 8. Long spacings d_L of various beidellite organic complexes and corresponding calorimetric measurements for the tetradecyl system.

Table 1. Transition data $\Delta S_i, T_i$ of kink block formation ($\Delta H_{theor} = 0.83\ \text{kcal}\cdot\text{mol}^{-1}, \Delta H_{exp} \approx 0.73\ \text{kcal}\cdot\text{mol}^{-1}$)

System	L_0/c	ΔS_1	T_1/°C	ΔS_2	T_2/°C	ΔS_3	T_3/°C
2×C18	18	2.54	56 (60)	2.47	65 (74)	2.43	70 (85)
2×C14	14	2.59 (2.3)	48 (47)	2.50 (2.3)	60 (58)	2.44 (2.3)	69 (70)
2×C10	10	2.66	40 (40)	2.53	57	2.44	

cross-section of a PE chain increases from 18.2 Å to 20.7 Å^2 during the transition from the all-trans to the new phase. This increase of about 15% is compensated partially by a shortening of the chains. From the change in cross-section and the 5% increase in specific volume[15,22] one calculates a chain shortening of about 10%. Looking for an energetically favoured chain conformation with a 10% shortening with respect to the trans chain, potential calculations suggest the structure in Fig. 9 with a period of 4.57 Å is in very good agreement with the shortened chain length of 4 CH_2-groups (4.6 Å).

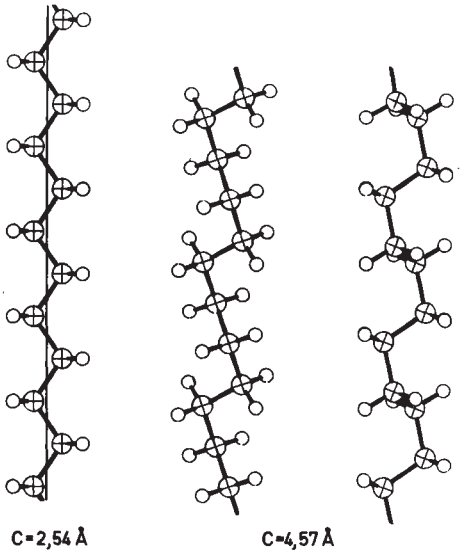

Fig. 9. Suggested ideal chain conformation in the high pressure phase of PE.

This suggested conformation can be described as a tgtḡtgtḡ-sequence but will only incorporate additional conformational entropy if transitions in the rotational potential are allowed. This together with a nearly perfect (i.e. crystalline) lateral packing of the chains can be achieved by virtue of the cluster-entropy hypothesis. In Fig. 10 some possible arrangements are built up with Stuart models which show a sufficiently good packing of adjacent chains if they have identical conformations and provided the chains are nearly straight, i.e. every second C–C-bond is in a trans-position. In the assembly at the lower right a crystal defect—a pair of holes—is shown which arise from a chain conformation differing from the adjacent ones. A statistical treatment of this laterally crystalline phase and of its formation from the all-trans crystal is readily achieved by using the C_2H_4-rotators as statistical elements (Fig. 11). Partition functions are now calculated—similar to the above treatment (Fig. 5)—for each rotator in the rotational potential of one of its adjacent C–C-bonds (1/2 of the above given $U(\varphi)$) specifically for the trans- and both gauche-conformations.

The free energy G of the system is composed of the respective molar free energies G_t and G_g multiplied by their probabilities and an additional entropy term $R \ln 2$, which takes into account the respective mirror images of the described microstates. The middle line of G(Fig. 11) gives the full entropy of mixing the trans and gauche states of the rotators taking into account the cluster-entropy hypothesis. The lower line comprises as before the cooperativity of the problem. The first two terms give the deformation energy due to the difference in cross-sections of the trans- and gauche-blocks, the last term takes into account the deformation energy which balances the fluctuation in chain length. All cooperative terms

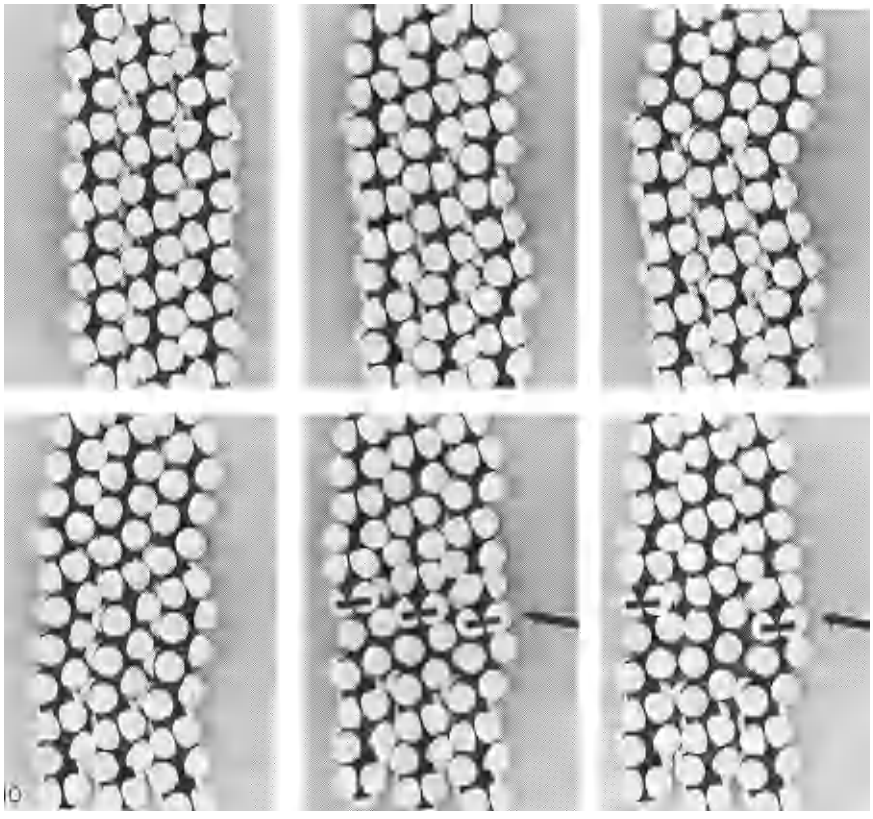

Fig. 10. Some possible arrangements of chains in the PE-high pressure phase.

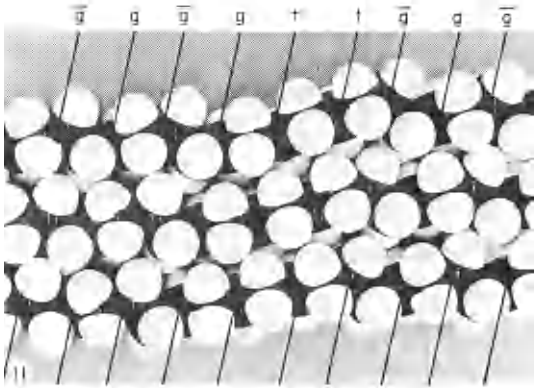

$$G = (1-y)G_t + yG_g + yp\Delta V - yRT\ln 2 + RT\left[y\ln y + (1-y)\ln(1-y)\right] + \frac{V_0}{2}\left[\frac{1-y}{\kappa_t}\left(\frac{\delta A}{A_0}\right)^2 + \frac{y}{\kappa_g}\left(\frac{\Delta A-\delta A}{A_0}\right)^2 + \frac{y(1-y)}{S_{cc}}\left(\frac{\Delta c}{c_0}\right)^2\right]$$

Fig. 11. Model describing the phase transition to the PE-high pressure phase and its related free energy per C_2H_4-rotator (y-probability for g or $\bar{g}$ conformation, $1-y$ for t-conformation). Full cluster-entropy assumed.

vanish in the limit of either all trans or all gauche conformations.

By applying the two equilibrium conditions

$$\frac{\partial G}{\partial \delta A} = 0, \quad \frac{\partial G}{\partial y} = 0 \tag{7}$$

one gets a similar formula as for the clay organic complexes (3)

$$\frac{G_g - G_t}{RT} + \frac{p\Delta V}{RT} - \ln 2 = \ln\frac{1-y}{y} + B(2y-1) \tag{8}$$

with the cooperativity parameter

$$B = \frac{V_0}{2RT}\left[\frac{1}{K}\left(\frac{\Delta A}{A_0}\right)^2 + \frac{1}{S_{cc}}\left(\frac{\Delta c}{c_0}\right)^2\right] \approx 10 \tag{9}$$

which is sufficiently large to get the full entropy and enthalpy difference during this first order transition. To calculate B the following data were used: $K = K_c = 2, \ldots, 0.8\times10^{-5}\,\text{bar}^{-1}$ for $p = 0, \ldots, 5$ kbar,[20] $S_{cc} = 3.4\times10^{-7}\,\text{bar}^{-1}$, $V_0 = 28\,\text{cm}^3$ (C_2H_4-rotator), $A_0 = 18.2\,\text{Å}^2$, $(\Delta A/A_0) = 0.15$, $(\Delta V/V_0) = 0.05$, $(\Delta c/c_0) = -0.10$.

The transition data of the new phase are the differences in entropy and enthalpy between the *tgtḡ* and the all-trans conformation, ΔH including the pressure work $p\Delta V$ and an additional energy contribution of 0.5 kcal/mol rotator, accounting for the less tight chain packing and corresponding to the 5% volume increase.

$$\Delta H_t = 0.62 + 0.5 + 0.034\,p/\text{kbar} \quad [\text{kcal/mole } C_2H_4] \tag{10}$$

$$\Delta S_t = 1.23 + 1.38 \text{ e.u.} \tag{11}$$

The interchain energy contribution (0.5) compares with potential calculations[21] of fitting kink pairs but must be still confirmed more accurately. These data together with the transition temperature and the volume effect are shown in Fig. 12 as functions of pressure (dashed curves, all data given per CH_2). The fully drawn curves in Fig. 12 approximate fairly close the experimental data for the total melting process, splitting up into the solid state transition (t) and the true melting at pressures above 3 kbar.

THE MELTING OF THE KINK-BLOCK PHASE

The interesting experimental fact, that for higher pressures a laterally crystalline phase consumes most of the enthalpy and entropy and more than half of the volume change during melting, in our opinion rules out, that in the subsequent melting any appreciable amount of coiling will take place. Although coiling can not be completely excluded at low pressures the analysis so far favours the bundle model for the molten state.

The final step, now, is to ask whether melting itself can be described, starting from the kink-block-phase discussed above. This is readily achieved, if one visualizes the large laterally crystalline kink-blocks to be broken into short fibrils by cooperatively incorporating packing

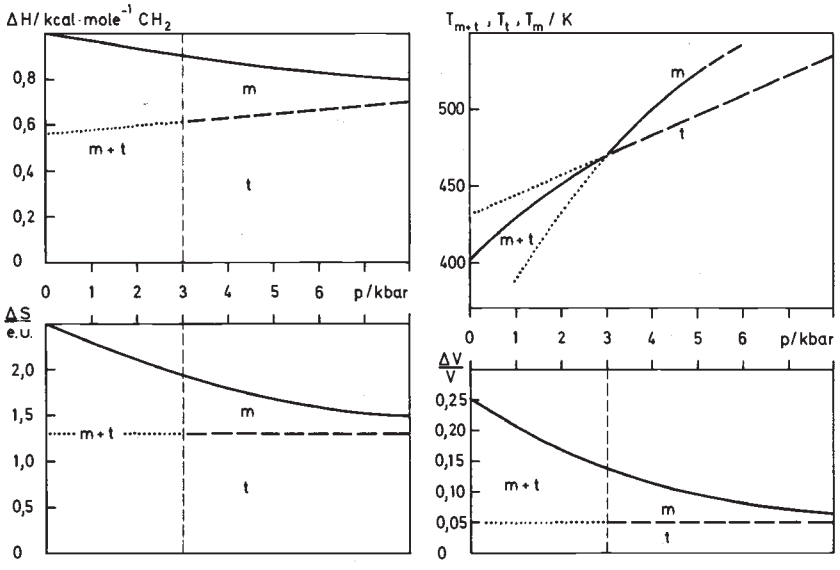

Fig. 12. Enthalpies, entropies, transition temperatures and volume changes for the solid state transition (dashed curves) and the melting of PE. The fully drawn curves give the sum of the respective quantities of both transitions.

irregularities (misfits) in between. The idea is, that such misfits form holes that carry energy as well as entropy, the latter because of their manyfold geometrical shapes determined by the various kink-blocks in the adjacent determined by the various kink-blocks in adjacent fibrils (Figs. 13, 14).

To describe the cooperative formation of holes in terms of accumulated misfits we first focus attention to neighbouring C_2H_4-rotators and remember, that there are one perfect (i.e. crystalline) and 3 imperfect pair conformations, enclosing misfits in each coordination. For simplicity we choose a coordination number 4, here. If z denotes the concentration of misfits in a growing hole between neighbouring chains, we may set up the free energy for a representative hole

$$G = z(\bar{U} + p\overline{\Delta V} - RT \ln 3) + RT\,[z \ln z + (1-z)\ln(1-z)] + \frac{V_0}{2S}\left(\frac{\overline{\Delta d}}{\bar{d}}\right)^2 z(1-z) \qquad (12)$$

with $\bar{U}$, $\overline{\Delta V}$ as mean energy and volume of a C_2H_4-rotator misfit in one lateral direction. The last term accounts for the cooperativity i.e. the deformation energy of bond angles necessary if misfits have not yet accumulated to give a sufficiently smooth hole. $\overline{\Delta d}$ characterizes the average additional chain separation in a misfit, S the compliance for sharp chain bending, which should not be much less than $S_{cc} = 3 \times 10^{-7}\,\text{bar}^{-1}$.

With this simple model one gets—in a similar thermodynamical treatment as above—a strong first order transition for the melting process but no information about the sizes of the generated holes. These must be approximately estimated from[21] (compare Fig. 13) and will be determined—together with their corresponding energies—by further semi-empirical potential calculations.

To procede further we now assume that $n = 4$ successive misfits compose a smooth hole (Fig, 13) and that one can subdivide all $\Omega = 3^n$ possible holes into 3 representative types, which are characterized by the following ΔV_i and U_i and degeneracies Ω_i

$$\Delta V_1/V_0 = 0.7 \quad \Delta V_2/V_0 = 1.0 \quad \Delta V_3/V_0 = 1.4$$
$$U_1 = 2.8 \qquad U_2 = 4.0 \qquad U_3 = 5.6\,\frac{\text{kcal}}{\text{mol}} \qquad (13)$$

and

$$\Omega_i = 3^n/3 = 27$$

$V_0 = 30\,\text{cm}^3$ is the molar volume of a C_2H_4-rotator in the kink-block phase. The ratio of hole energy to volume has been kept constant according to Ref. 21. The transition data at melting depend upon the concentrations c_i of holes being cooperatively formed. It seems obvious and takes into account the equilibrium state of the melt, that c_i must obey the usual Boltzmann distribution:

$$c_i = \frac{\Omega_i \exp\left[-\dfrac{U_i + p\Delta V_i}{RT}\right]}{1 + \sum_i \Omega_i \exp\left[-\dfrac{U_i + p\Delta V_i}{RT}\right]}. \qquad (14)$$

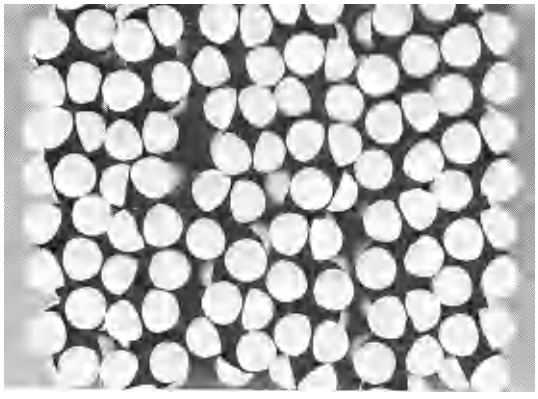

Fig. 13. Kink-block-phase broken into fibrils by smooth holes which originate from cooperatively arranged misfits between neighbouring rotators (longitudinal section).

The entropy and enthalpy of melting and volume change are given by

$$\Delta S_m = \frac{2}{8} R \ln 3^4 \times \sum c_i + \delta S \quad \text{e.u./mol CH}_2 \qquad (15)$$

$$\Delta H_m = \frac{2}{8} \sum c_i (U_i + p\Delta V_i) + \delta H \quad \text{kcal/mol CH}_2 \qquad (16)$$

$$\Delta V_m = \frac{2}{8} \sum c_i \Delta V_i. \qquad (17)$$

These data refer to one CH_2-group (8 CH_2-groups per hole length). The factor 2 accounts for the two independent coordination directions (Fig. 14). The small additional terms $\delta S = 0.08$ e.u. and $\delta H = 0.02$ kcal/mol take into account entropy and energy of the meander superstructure.[3] The results of (15–17) are added to the

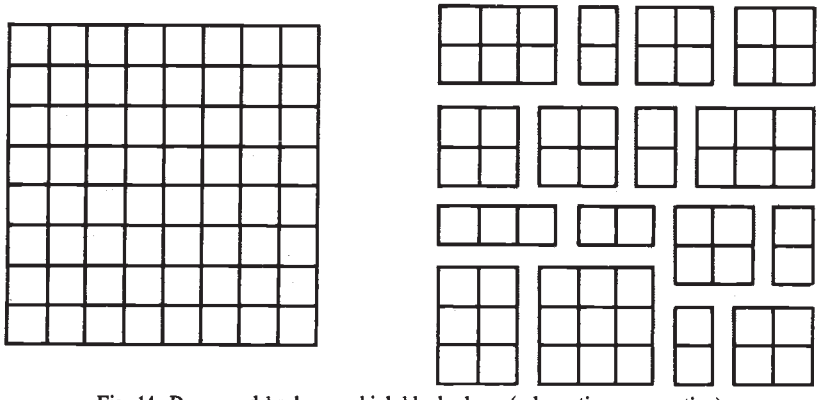

Fig. 14. Dense and broken up kink-block-phase (schematic cross-section).

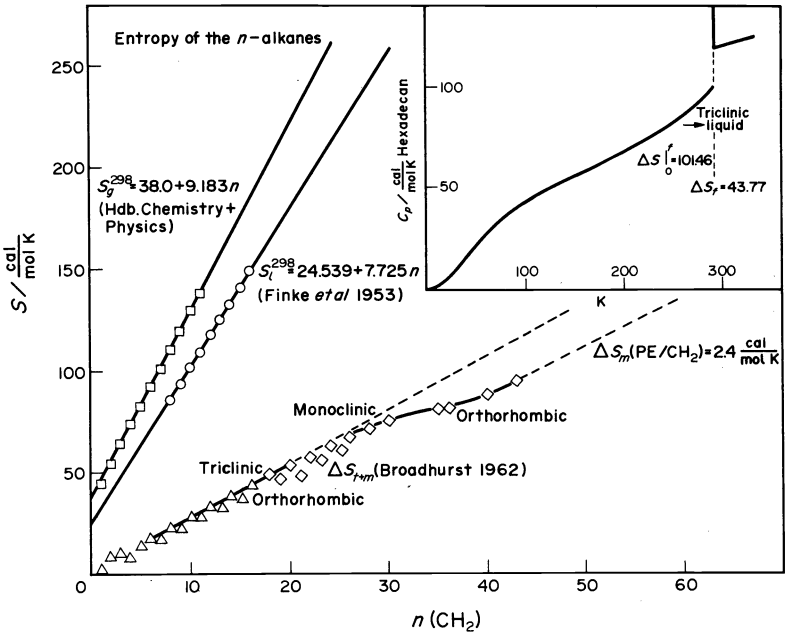

Fig. 15. Summary of entropy data of the n-alkanes from various sources.

corresponding data of the kink-block transition and plotted in Fig. 12 as fully drawn curves. They fit the experimental data sufficiently.

The temperatures of melting are calculated by

$$T_m = \frac{\Delta H_m}{\Delta S_m}$$

(data from 15, 16) above 3 kbar and

$$T_{m+t} = \frac{\Delta H_t + \Delta H_m}{\Delta S_t + \Delta S_m}$$

(data from 10, 11 and 15, 16) below 3 kbar, i.e. in the region where T_t would be above T_m.

CONCLUSION

An improved version of the bundle model allows a quantitative discussion of the solid state transition and the final melting of PE. It is possible to calculate the transition data as well as the cooperativity. A similar quantitative treatment can also be given for 1.4-trans-PBD, which is a little more complicated geometrically because of the one cis and two skew valleys of the rotational potential.

The question, whether coiling of molecules occurs in the melt can be negated for high pressures but cannot be finally answered for the low pressure region—from these considerations—without a similar treatment of interpenetrating coils which seems to be very difficult.

Figure 15 shows a summary of entropy data for the n-alkanes from various sources. If one compares the slopes of the entropy-curves for the liquid and the gaseous state at 298 K there is a difference of 1.46 e.u. per CH_2 which at least partially may be due to the subsequent coiling of molecules during evaporation. This argument, we believe, favours the bundle concept of the liquid phase too.

Acknowledgement—The authors would like to thank the Deutsche Forschungsgemeinschaft for various financial supports.

REFERENCES

[1]P. J. Flory, Principles of polymer chemistry, Cornell Univ. Press, N.Y. (1953); Statistical mechanics of chain molecules N.Y. (1969).
[2]Th.G. F. Schoon, *Proc. Int. Rubber Conf.* 277 (1967).
[3]W. Pechhold, M. E. T. Hauber and E. Liska, *Kolloid Z.u.Z. Polymere* **251**, 818 (1973).
[4]V. A. Kargin, A. I. Kitajgorodskij and G. L. Slonimskij, *Kolloid-Zh.* **19**, 131 (1957);*Colloid J. USSR* **19**, 141 (1975).
[5]G. S. Y. Yeh, *J. Macromol. Sci.* **B6**, 465 (1972).
[6]B. Vollmert and H. Stutz, *Angew. Makrom. Chemie* **3**, 182 (1968); **25**, 187 (1972).
[7]J. Schelten, W. A. Kruse and R. G. Kirste, *Kolloid Z.u.Z. Polymere* **251**, 919 (1973).
[8]J. Schelten, G. D. Wignall, D. G. Ballard and W. Schmatz, *Colloid and Poly. Sci.* **252**, 749 (1974).
[9]J. H. Wendorff, E. W. Fischer, K. Dransfeld, G. Margret and M. Schickfuss, *Verhandl. DPG* **10**, 444 (1975).
[10]W. Pechhold and M. E. T. Hauber, in preparation
[11]J. Petermann and H. Gleiter, *Phil. Mag.* **28**, 1279 (1973).
[12]J. Petermann and H. Gleiter, *Phil. Mag.* **31**, 929 (1975).
[13]J. Petermann and H. Gleiter, *J. Macromol. Sci.* In press.
[14]S. Blasenbrey and W. Pechhold, *Ber. Bunsengesellschaft Phys. Chemie* **14**, 184 (1970).
[15]D. C. Bassett and B. Turner, *Phil. Mag.* **29**, 925 (1974).
[16]D. C. Bassett, S. Block and G. J. Piermarini, *J. Appl. Phys.* **45**, 4146 (1974).
[17]G. Lagaly, S. Fitz and A. Weiss, *Prog. Colloid and Polymer Sci.* **57**, 54 (1975).
[18]G. Lagaly, S. Ritz and A. Weiss, *Clays and Clay Minerals*, **23**, 45 (1975).
[19]G. R. Strobl, *Habilitationsschrift*, Mainz (1975).
[20]T. Hatakeyama, T. Hashimoto and H. Kanetsuna, *Colloid and Polymer Sci.* **252**, 15 (1974).
[21]P. C. Hägele, G. Wobser, W. Pechhold and S. Blasenbrey, *IUPAC-Symp.* Boston (1971).
[22]U. Leute, W. Dollhopf and E. Liska, *Colloid and Polymer Sci.* In press.